This article has been accepted for publication in IEEE Transactions on Transportation Electrification. This is the author's version which has not been fully edited and content may change prior to final publication. Citation information: DOI 10.1109/TTE.2024.3399329

TTE-Reg-2024-01-0166

Modular MV Naturally Balanced Converter with High-Frequency Isolation and no DC-Link Capacitor for EV Fast Charging

Andrei Blinov, *Senior Member, IEEE*, Andrii Chub, *Senior Member*, *IEEE*, Naki Guler, *Senior Member*, *IEEE*, Sertac Bayhan, *Senior Member, IEEE, Leila Parsa, Fellow, IEEE,* and Dmitri Vinnikov, *Fellow, IEEE*

***Abstract*—This paper presents and verifies the concept of a converter for a medium voltage (MV) electric vehicle (EV) charging station that employs high-frequency galvanic isolation and features no dc link capacitor. The system is based on multi-cell boost (MCB) topology; however, instead of a conventional two-stage configuration with dc link, isolated current source converter (iCSC) based cells are used. They perform power factor correction (PFC) while also providing HF galvanic isolation and are connected in series at the input and in parallel at the output. The exceptional feature of such configuration lies in inherent voltage balancing among the cells, which significantly simplifies the control and protection and improves scalability. The concept is verified with a scaled 4 kW prototype having three iCSC cells.**

***Index Terms*— electric vehicle (EV) charger, off-board charger (OBC), power factor correction (PFC), single-stage AC-DC converter.**

I. Introduction

TRANSITION to electrified transport is increasing at its pace, with more and more manufacturers entering the electric vehicle (EV) market. There is a high probability that this trend will only speed up, instigated by various governmental initiatives. These include the EU plan for making all new cars sold in the EU to be zero-emission vehicles starting in the year 2035 and the US goal to make half of light trucks sold in the U.S. in 2030 be zero-emission vehicles or including plug-in hybrids [1],[2]. In this context, the satisfaction of EV user expectations in terms of refueling time and availability of charging infrastructure are of major importance. To address this, a range of initiatives and roadmaps were launched to increase the number of charging points per EV and road distance. Today, the chargers are typically installed at EV users' private houses, on parking lots, or along roads and highways and the charging stations market is projected to have sustained growth in the following years [3]. A significant part of new installations is expected to be represented by fast charging stations (FCS) with charging times of 8 minutes / 100 kilometers [4], [5]. These stations provide dc current and bypass the low-power ac-dc on-board charger of the vehicle (see Fig. 1)

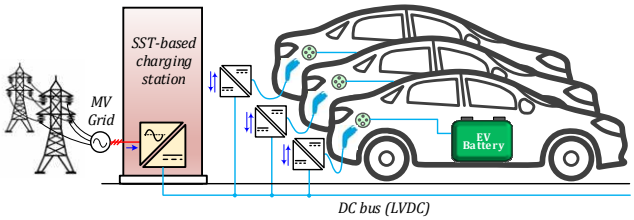


Fig. 1 Generalized representation of fast charging station with dc-bus supplied from MV three-phase grid.

To improve the technology of high-power charging infrastructure, many studies have been directed toward novel solutions for fast charging stations. This paper proposes a novel modular concept based on isolated current source converter (iCSC) cells. In contrast to most similar systems, it features no dc link capacitor and provides the unique property of natural voltage balancing among the cells. These properties can provide remarkable advantages in terms of implementation complexity, redundancy, scalability, and cost. The content is organized as follows: Section II gives an overview of existing solutions for fast EV charging stations and their challenges; Section III describes the proposed solution; Section IV gives design considerations; the experimental verification is presented in Section V; finally, the paper is concluded in Section VI.

II. Existing Solutions for MV Charging Stations

A. Topologies for MV Applications

Presently, systems used in fast dc charging stations are generally supplied from medium voltage (MV) ac grids to ensure the required power capacity. The voltage step-down from MV to LV used by the power electronics is generally provided by a line frequency (LF) transformer that is located

Manuscript received January 23, 2024; revised March 19, 2024; Accepted April 22, 2024. This work was supported in part by the project NPRP12S-0214-190083 from the Qatar National Research Fund (a member of Qatar Foundation), in part by the Estonian Research Council grant PRG1086 and in part by the Estonian Centre of Excellence in Energy Efficiency, ENER (grant TK230) funded by the Estonian Ministry of Education and Research.

The review of this article was coordinated by

Andrei Blinov, Andrii Chub and Dmitri Vinnikov are with the Electrical Power Engineering and Mechatronics Department, Tallinn University of Technology, Tallinn, 12616, (e-mail: andrei.blinov@taltech.ee; andrii.chub@taltech.ee; dmitri.vinnikov@taltech.ee).

Naki Guler and Sertac Bayhan are with the Qatar Environment and Energy Research Institute, Hamad Bin Khalifa University, Doha, 34110, Qatar (e-mail: sbayhan@hbku.edu.qa)

L. Parsa is with the Department of Electrical Engineering, University of California, Santa Cruz, CA 95064 USA (e-mail: lparsa@ucsc.edu).

Digital Object Identifier

This work is licensed under a Creative Commons Attribution 4.0 License. For more information, see https://creativecommons.org/licenses/by/4.0/

This article has been accepted for publication in IEEE Transactions on Transportation Electrification. This is the author's version which has not been fully edited and content may change prior to final publication. Citation information: DOI 10.1109/TTE.2024.3399329

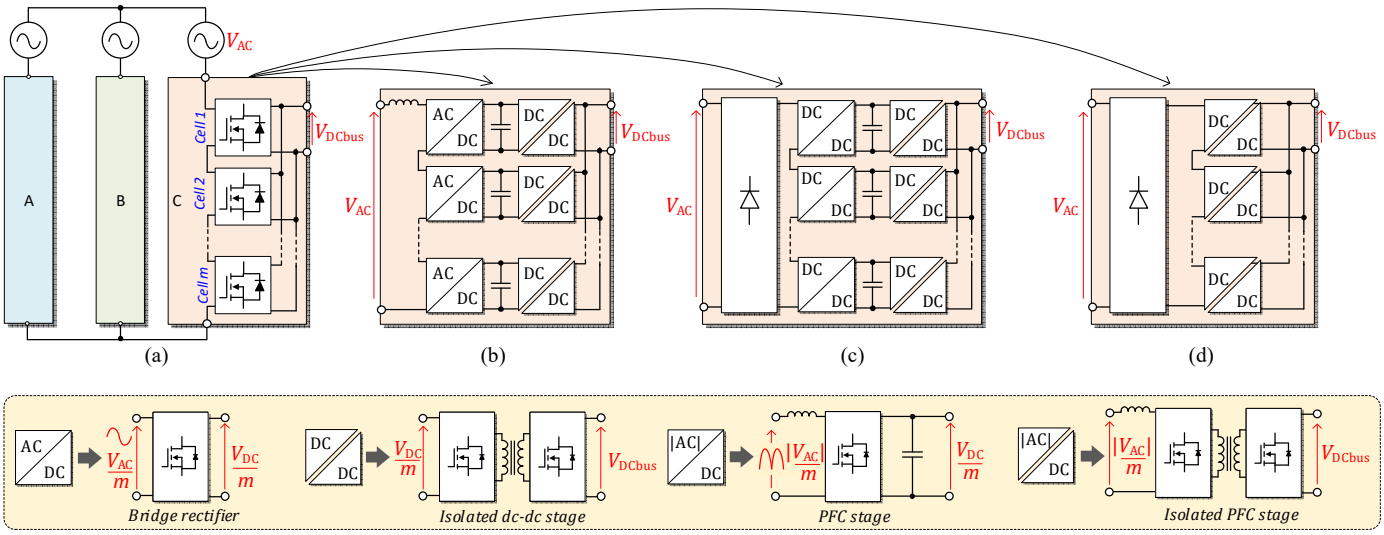


Fig. 2 Modular MV converter with ISOP configuration of cells (a); two-stage topology with ac-dc rectifier and isolated dc-dc converter in each cell (b); two-stage topology with common input side rectifier and converter cells containing a dc/dc boost PFC stage and isolated dc-dc converter stage (MCB); proposed single-stage configuration based on MCB topology with common input side rectifier and isolated current-source converters (d).

(typically in a separate structure) near the charging site [6]. To reduce the volume and weight of the installation, some innovative FCS concepts are taking advantage of modular systems with high-frequency (HF) transformers and can be referred to as solid-state transformer (SST) based fast chargers [7],[8],[9],[10].

One of the ways to provide connection to MV is to utilize high-voltage power semiconductors with multilevel topologies, such as 13 kV SiC MOSFETs in [11], that are used for the input voltage of 3.6 kVAC. Still, the obtainable input voltage is confined due to limitations in semiconductor technology. Alternatively, the semiconductor valve can be composed of series-connected devices that share the total voltage applied [12]. Other SST configurations generally assume multiple cells (sub-modules) in input-series output-parallel configuration (Fig. 2a). Thanks to a typically large number of cells, many voltage levels, and higher operating frequencies, such solutions require reduced line inductor ratings.

Among various configurations, the multi-cell boost (MCB) topology offers the advantage of reduced total semiconductor ratings and higher efficiency [7]. The MCB charger can be realized in a few ways, depending on application requirements and preferences. For example, the rectifier can be realized using a common (diode) bridge circuit or individual rectifiers inside each cell (see Fig. 2b and c) [8]. Likewise, either the single line inductor can be used, or the required inductance could be distributed among cells [9]. Furthermore, a multi-winding transformer can be employed to provide extra flexibility and possible cost benefits [13].

Most state-of-the-art MCB configurations assume a two-stage configuration with an intermediate dc link. One of the popular solutions for MV charging converter [10] was realized with a three-level PFC boost rectifier stage, interfaced with a three-level neutral point clamped (3L-NPC) converter through intermediate dc-link in [14]. The concept uses only film capacitors and offers high efficiency and reduced weight. Still, since the dc link is used to filter the line frequency component from the input of the second stage, it usually results in a part that contributes significantly to the cell volume and presumably also the overall cost of the system.

The potential way to address the mentioned drawback of MCB configuration is to apply a single-stage topology configuration without the dc link. The concept of a multilevel converter composed of cells that are based on isolated matrix converters (IMC) was presented in [15]. Such converters use bidirectional switches made of anti-series connection of discrete semiconductors. Due to many devices connected in series at the grid side performing ac-ac conversion, the modulation and control are quite complex. To address this, a semi-modular SST was proposed in [16]. It features a common diode bridge rectifier, similar to standard MCB topology. However, instead of a two-step conversion through stabilized dc-link, a single-stage conversion using dual half-bridge (DHB) topology is employed. As a result, the number of components is reduced compared to the IMC-based solution, while the bulky dc link is similarly omitted. At the same time, the PFC operation of the DHB converter is associated with several compromises related to input current regulation as well as input voltage and power balancing. As a result, the system requires many sensors, a complex modulation scheme and communication channels between the cells.

B. Challenges of Voltage Balancing.

In conventional modular dc-dc ISOP systems based on widely used topologies, such as dual active bridge (DAB), the power and voltage balancing between the modules is a very challenging and complex topic. An extra balancing controller is typically required, and the solutions implemented can vary from straightforward centralized to sophisticated ones involving learning-based methods [18]. Typically, each module requires information from several references and

This work is licensed under a Creative Commons Attribution 4.0 License. For more information, see https://creativecommons.org/licenses/by/4.0/

This article has been accepted for publication in IEEE Transactions on Transportation Electrification. This is the author's version which has not been fully edited and content may change prior to final publication. Citation information: DOI 10.1109/TTE.2024.3399329

TTE-Reg-2024-01-0166

TABLE II
COMPARISON OF SST-BASED MODULAR CONVERTERS

Ref	Isolation	Topology	DC-link	Rectification	Cell-level sensing	Transmitted signals	Comments
[6]	LF+HF	CFPP	Pulsating	Module-level	N/A	N/A	Based on LF transformer, followed by isolated ac-dc cell with interleaved phases; centralized PWM
[15]	HF	IMC	Absent	Cell-level	N/A	N/A	Input-series output parallel connected isolated matrix converters; local PWM generation.
[10]		MCB	Bulky		None	All PWM	3L-boost + stacked LLC with centralized PWM. No cell-level measurement; balancing from <1% component parameter mismatch
[9]					V_{DC}, I_{OUT}	V_{DCref}, Mod, I_{OUTref}	PSFB with cell-level rectification; decentralized PWM
[14]				Common	V_{DC1}, V_{DC2}	All PWM	3L-boost + 3L-NPC with common rectification; centralized PWM with fiber optic cables.
[16]			Pulsating		V_{DC}, I_{DC}, V_{OUT}	Grid angle, I_{ACref}, V_{INref},	DHB with common rectification; decentralized PWM
Proposed					I_{DC}	Grid angle, I_{ACref}	iCSC with common rectification; decentralized PWM with minimal cell-level sensing and natural balancing

*PSFB – *iCFPP – interleaved current-fed push-pull, IMC – isolated matrix converter, PSFB – phase shifter full-bridge, 3L- three-level, NPC – neutral point clamped, DHB – dual half-bridge.

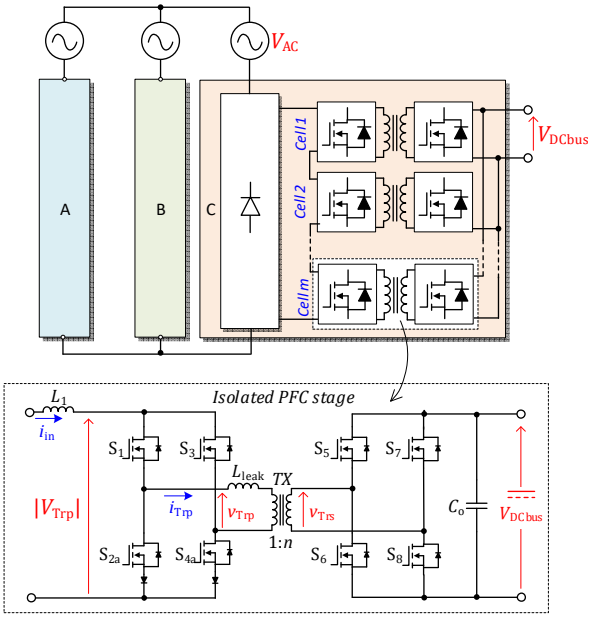


Fig. 3 Proposed MCB with current source cell topology based on full-bridge ASMC.

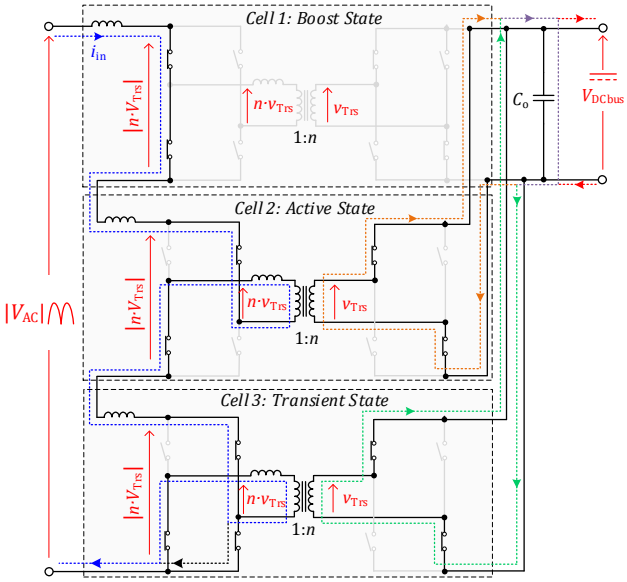


Fig. 4 Representation of current flows and voltage sharing on the example of three cells in different switching states: the bridges of iCSCs continuously maintain the path for the input current flow due to $D_{AC} > 0.5$.

sensors [19]. For example, in the PSFB-based system from [14], each cell needs to be sensing two dc-link voltages, while also having a centralized generation of PWM signals that are transferred by a high-bandwidth optical interface. Moreover, in the case of a fault in one cell, additional control measures need to be taken to balance the input voltage between the remaining operational cells. The requirement of many sensors and communication between the cells, as well as the high computational burden, are affecting the cost of the MV FCS system. Such solutions are lacking in terms of scalability and can be considered for systems with a relatively low number of cells. The comparison of properties of various SST-based systems is presented in Table I.

In this paper, a novel configuration is proposed by utilizing a single-stage iCSC topology without the intermediate dc-link (Fig. 2d), which provides PFC and galvanic isolation simultaneously and with natural voltage balance among the cells [17].

III. PROPOSED SINGLE-STAGE MCB WITH CSCS

A. Natural voltage balancing

To improve scalability and reduce complexity, while keeping the advantages of single-stage MCB, the use of iCSC in each cell is proposed in this paper (Fig. 2d). In general, most of the iCSC topologies can be applied as cells in the MCB converter. The comparative analysis of example topologies is given in [17]. These converters typically implement zero current switching (ZCS) techniques to mitigate the voltage spike at switch turn-OFF. In the frame of this study, the asymmetric secondary-modulated converter (ASMC) shown in Fig. 3 is used as the basic cell.

This work is licensed under a Creative Commons Attribution 4.0 License. For more information, see https://creativecommons.org/licenses/by/4.0/

This article has been accepted for publication in IEEE Transactions on Transportation Electrification. This is the author's version which has not been fully edited and content may change prior to final publication. Citation information: DOI 10.1109/TTE.2024.3399329

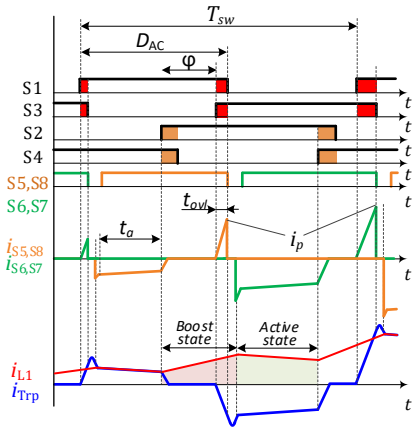


Fig. 5 Generalized operating principle of ASMC.

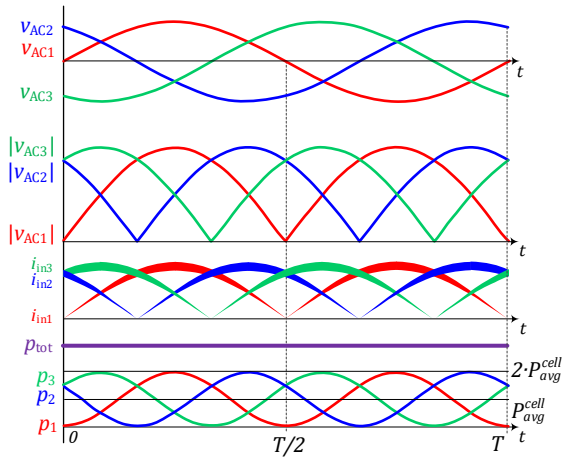


Fig. 6. Generalized operating principle of three-phase MCB converter without dc link: by connecting all three phases at the output, the pulsation of each is compensated, providing continuous dc power.

The key feature of implementing iCSC lies in inherent voltage balancing across the cells. Due to the nature of typical CSC, at least two transistors in the input bridge circuit are always conducting, creating a continuous path for the current. The same is true for multiple iCSC cells connected in series – they all would share the same input current, regardless of whether interleaving is used, as shown in Fig. 4.

The steady-state level of the primary transformer voltage of the ASMC is equal to the reflected voltage value from the secondary side. As the secondary windings are connected in parallel, identical voltage values would appear on the primary windings of the series-connected cells (multiplied by the turns ratio). Thus, the voltage balance is achieved naturally, without the need for external circuits or control loops. This is the distinguished property of ISOP-connected iCSCs, that does not appear in voltage-source topologies.

$$\begin{cases} I_{\mathrm{AC}}\left|\sin(\omega\cdot T)\right| = I_{\mathrm{L1}}\left|\sin(\omega\cdot T)\right| \\ \left|V_{\mathrm{Trp}}\right| = \left|V_{\mathrm{Trs}}\right| / n = V_{\mathrm{DCbus}} / n \\ V_{\mathrm{IN}}\left|\sin(\omega\cdot T)\right| = \dfrac{V_{\mathrm{AC}}\left|\sin(\omega\cdot T)\right|}{m} \end{cases} \quad (1)$$

where T is the grid frequency period, I_{AC} is the magnitude of the input current, I_{L1} is the magnitude of the cell inductor current, V_{Trp} is the transformer primary voltage maximum value, V_{Trs} is the transformer secondary voltage amplitude value, n is the transformer turns ratio and m is the number of ISOP-connected cells.

The ISOP connection of current-source dc-dc converters for MVDC applications was verified in [20] and showed exceptionally good voltage-sharing properties and fault-tolerant operation capability. Such a system achieves power and voltage sharing naturally and does not require complex balancing efforts as the DAB-based counterparts do. Moreover, the ISOP-connected iCSCs demonstrate remarkable fault-tolerant operation. In [20], to obtain interleaved operation of iCSCs, the clock of the cells was synchronized by using the same microcontroller. The requirement of interfaces between the cells negatively impact the cost of the system and may also impose additional restrictions on long-term reliability. In the proposed concept, the motivation of the authors is to keep the number and requirements of the cell's I/O signals to a minimum. Thus, despite the apparent advantage of interleaved operation, the operation without this feature was assumed in this paper. This way, each cell will require only a limited amount of low-bandwidth communication signals.

Due to the absence of dc-link, the output current of each cell has instantaneous output power pulsations of twice the grid frequency, varying between zero and two times the average. The generalized representation of the operation is illustrated in Fig. 6. It should be noticed that the full charging station is considered to have a three-phase input connection (see Fig. 1). If the dc outputs from all phases are connected in parallel, the problem of this second harmonic will be eliminated and no significant filtering efforts will be required.

B. Current Source Converter-based cell

In this study, each cell is composed of iCSC based on ASMC converter in Fig. 3. The topology was originally introduced in [21] for dc-dc application, and its modulation principle is presented in Fig. 5. Despite specific modulation ensuring ZCS conditions, the general characteristics of the converter are similar to those of conventional boost PFC one [22]. The advantages include constant operating frequency, low current circulation, reduced switching losses, and bidirectional operation capability (in case such a mode is required in some embodiments). Otherwise, the topology can be substituted, for example, by the unidirectional version – asymmetric resonant converter [23]. It shares the advantages of ASMC but cannot regulate the value of peak current, thus resulting in slightly higher energy circulation in the top bridge devices and transformer.

To provide PFC, the ASMC topology uses a special phase-shift modulation (PSM) technique to provide ZCS for the primary devices and avoid a large voltage spike across them (Fig. 7). The primary devices are operating with a duty cycle higher than 0.5 to avoid open circuit condition for the

This work is licensed under a Creative Commons Attribution 4.0 License. For more information, see https://creativecommons.org/licenses/by/4.0/

This article has been accepted for publication in IEEE Transactions on Transportation Electrification. This is the author's version which has not been fully edited and content may change prior to final publication. Citation information: DOI 10.1109/TTE.2024.3399329

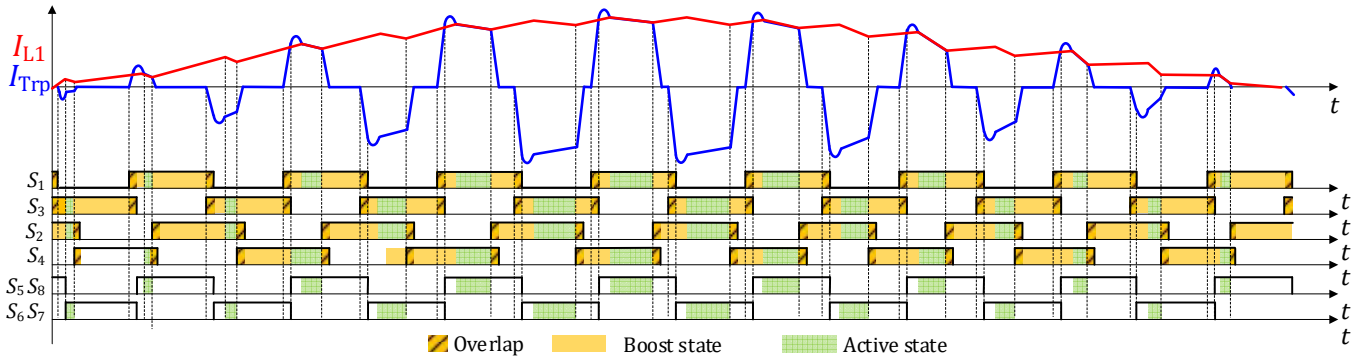


Fig. 7. Generalized representation of the ASMC cell modulation sequence over one-half on the grid period.

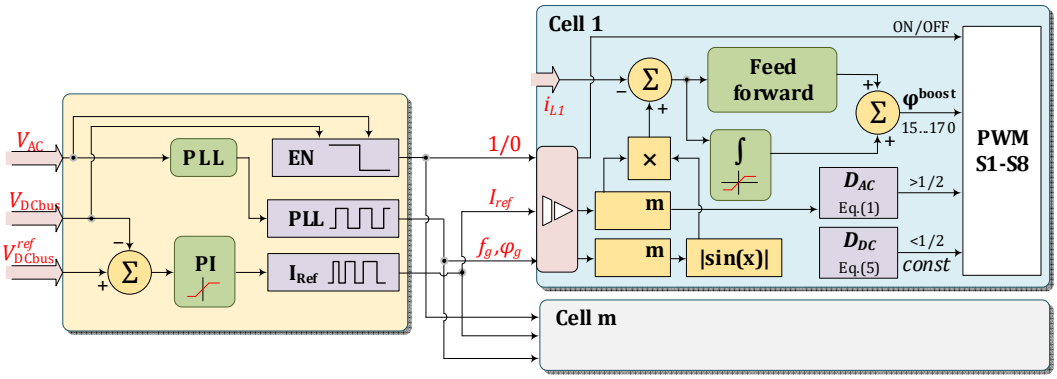


Fig. 8. Simplified control of the modular converter with reduced number of communication links.

current path. The duty cycle depends on the transformer leakage inductance and is chosen such that:

$$D_{\mathrm{AC}} > \frac{1}{2} + \frac{2 \cdot n \cdot i_{\mathrm{L1}} \cdot L_{leak} \cdot f_{sw}}{V_{\mathrm{DCbus}}}, \tag{2}$$

where f_{sw} is the switching frequency, L_{leak} is the transformer equivalent leakage inductance.

To minimize the energy circulation, a variation of the duty cycle of the transistors S_1 and S_2, together with instantaneous current value, is introduced.

The input current is regulated by controlling the phase shift of bottom switches in the primary bridge related to other switches. Since a certain time is necessary for establishing the ZCS condition, the minimal and maximal phase shift angles should be defined. Neglecting the influence of the quasi-resonant interval, they can be estimated as:

$$\varphi_{\min} \approx \frac{4 \cdot \pi \cdot f_{sw} \cdot n \cdot L_{leak} \cdot i_p}{V_{\mathrm{DCbus}}} \tag{3}$$

$$\varphi_{\max} \approx \pi - \frac{2 \cdot \pi \cdot f_{sw} \cdot n \cdot L_{leak} \cdot i_{L1}}{V_{\mathrm{DCbus}}} \tag{4}$$

where i_p is the time-varying peak current flowing in the top transistors S_1 and S_3 and i_{L1} is the instantaneous input current.

IV. Design Considerations

A. Component Selection

Thanks to its modular structure, the proposed MCB configuration can theoretically be suited for any MV level. In practice, the voltage of the cell can be chosen to allow using commercial 650…1700 V high-performance semiconductors, like SiC MOSFETs or JFETs. At the same time, it is worth mentioning that each transformer of the MCB converter cell should withstand the full input MV level of the system. As a result, the isolation is estimated to occupy a larger part of the transformer window and the overall volume of transformers will be higher than that of other competitive MV charger configurations [7].

One of the main peculiarities of iCSCs is associated with voltage overshoots. This problem can be mitigated using snubber/clamping circuits, topology modifications, resonant switching, or modulation techniques. However, the oscillations caused by semiconductor capacitance and leakage inductance generally remain [24]. As a result, iCSCs typically require slightly higher voltage-rated devices than VSCs of equal voltage levels. To reduce this effect, the iCSC transformers are typically designed with a minimal leakage inductance value. Since most of the EVs have nominal battery voltages of around 400 V or 800 V, the level of the output voltage can be adjusted by dividing the secondary windings into groups and arranging them in series and/or parallel. Alternatively, the output voltage can be adjusted by connecting the dc-dc cells with a switching matrix of high-power relays. To facilitate obtaining the design with minimized leakage inductance, the transformer should preferably have a relatively low turns ratio, which is quite easy to achieve considering the semiconductor voltage range discussed earlier.

B. Communication and Control System

In modular systems, reaching the desired voltage and power balancing between the cells is among the highest priorities. In

This work is licensed under a Creative Commons Attribution 4.0 License. For more information, see https://creativecommons.org/licenses/by/4.0/

This article has been accepted for publication in IEEE Transactions on Transportation Electrification. This is the author's version which has not been fully edited and content may change prior to final publication. Citation information: DOI 10.1109/TTE.2024.3399329

MV systems, the isolation requirement for sensing and communication can significantly affect the feasibility of the solution. Not only does it increase the complexity of the converter and its cost, but long-term reliability and running costs are also affected, as such systems are typically expected to be located outside.

To operate in closed-loop mode, each cell requires limited information about the system. One of the ways would be to simultaneously send the same estimated duty cycle (or phase shift) value to every cell from a master module, which is generated based on phase-locked loop (PLL) and inner/outer control loops. In practice, that would require transmission of the signal with a relatively high bandwidth. An alternative approach would be to address the component parameter mismatch and obtain better controllability of the current inside each cell by locating the current sensor and control loop inside the cell. The master module would then provide the PLL and current reference signals to each cell. This way, only the signals with relatively low bandwidth should be transmitted, which can relax the hardware requirements and reduce the costs.

The implemented control principle is presented in Fig. 8. The master module includes input and output voltage sensors and is responsible for PLL and current reference for the cells. It can also incorporate protection and external communication. The grid angle and frequency are transferred to each cell through isolators as a 50% duty ratio signal at grid frequency, while the current reference – by 1 kHz PWM signal with 10…90% variable duty ratio referring to minimal and maximal input currents, respectively.

The obtained signals are converted to sinusoidal/variable references by the corresponding math blocks inside each cell. Readings from the local current sensor are used to estimate the input current error. The cell control system is based on a combination of feedforward and integral regulators. The feedforward term estimates the required duty cycle value based on characteristics of the topology that are similar to that of a standard boost PFC converter.

Assuming ideal components, the input current i_{in} at time t+1:

$$i_{\text{L1}}(t+1) = i_{\text{L1}}(n) + \frac{v_{\text{AC}}(t)}{m \cdot L_{\text{tot}}} \cdot T_{sw} - \frac{V_{\text{DCbus}}(t)}{n \cdot L_{\text{tot}}} \cdot \left(1 - D_{FF}(t)\right) \cdot T_{sw} \quad (5)$$

where D_{FF} is the feedforward duty cycle, T_{sw} is the switching period, v_{ac} is the instantaneous value of the grid voltage and V_{DCbus} is the value of the output dc voltage, m is the number of ISOP-connected cells.

Assuming that the input current reference i_{ref} equals

$$i_{ref}(t) = I_{ref} \left|\sin(\omega \cdot T_{sw})\right|, \quad (6)$$

the duty cycle D_{FF} from (1) can be derived as

$$D_{FF}(t) = \left(1 - \frac{v_{\text{AC}}(t) \cdot n}{V_{\text{DCbus}}(t) \cdot m}\right) + \left(\frac{m \cdot L_{\text{tot}} \cdot \left(i_{ref}(t+1) - i_{ref}(t)\right)}{V_{\text{DCbus}}(t) \cdot T_{sw}}\right). \quad (7)$$

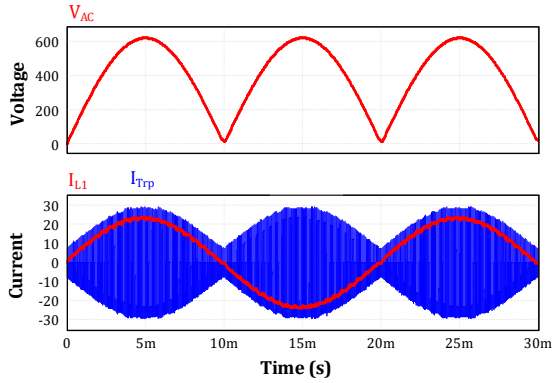


Fig. 9. iCSC input voltage and current as well as transformer primary current.

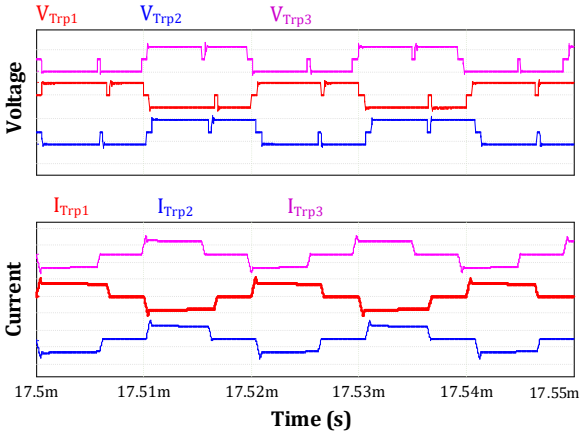


Fig. 10. Voltages and currents of iCSC transformers.

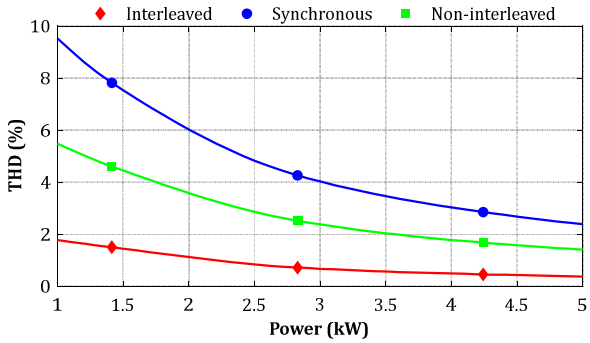


Fig. 11. Estimated THD of 3-cell CS-MCB operating with different modes (L_{tot}=1.35 mH).

Here, the first term is determined by the characteristic of the boost converter, while the second one is the inductor current forcing component.

As shown in the previous analysis, to implement soft switching, the iCSC should exhibit several transition modes, which results in duty cycle loss for the active state. To address this, the integral term is added to adjust the effect of the duty cycle loss, losses in components, input and output voltage variations, as well as other relevant factors:

$$D(t) = D_{FF} + D_{\text{I}} \quad (8)$$

The integral term D_{I} can be determined according to the guidelines from [25]. The resulting phase shift value is used to control transistors S_2 and S_4. To reduce energy circulation, the

This work is licensed under a Creative Commons Attribution 4.0 License. For more information, see https://creativecommons.org/licenses/by/4.0/

This article has been accepted for publication in IEEE Transactions on Transportation Electrification. This is the author's version which has not been fully edited and content may change prior to final publication. Citation information: DOI 10.1109/TTE.2024.3399329

duty cycles of transistors S_1 and S_3 vary, dependent on the instantaneous value of the current, while the duty cycles of other transistors are constant.

The simulated PFC operation of MCB made of three iCSC cells without interleaving is presented in Fig. 9. As observed, thanks to D_{AC} variation of top devices, the transformer current follows the input current with minor energy circulation. The voltage balance is demonstrated in Fig. 10 on the example of transformer primary voltages and currents using the PSIM model. As follows, using such relatively simple partially decentralized control, it is possible to provide balanced operation of cells with a minimal number of local sensors and communication links.

V. Experimental Verification

To verify the concept in the laboratory conditions, a scaled version of the MCB converter was designed. The 4 kW system consists of 3 cells and is supplied from a 440 V rms ac source (see Fig. 12). The parameters and main components are listed in Table II. As the full-scale system is assumed to be based on SiC semiconductors, this technology was used for the scaled prototype as well. Although this results in the use of significantly voltage-overrated devices, this decision was made to keep the properties of the technology (e.g. body diode reverse recovery) closer to the ones assumed for the full system. To obtain the reverse blocking capability of the transistors S_2 and S_4 and minimize losses, they were composed of anti-series connection of MOSFETs and driven with synchronous rectification.

The MCB structure allows the use of individual inductances inside each cell to form the line inductor, following the modularity principle. As the interleaving approach is not utilized in the prototype, the inductance value was chosen such that the average THD is below 5% at powers above ¼ rated. The estimated characteristics are shown in Fig. 11. As observed, the resulting THD for non-interleaved operation is in between the optimally interleaved (considering phase shift $\delta_{ph}=2\cdot\pi/m$) and synchronous (i.e., when all cells switch simultaneously $\delta_{ph}=0$) modes.

To keep the output voltage of the prototype similar to that of the full system, the use of a step-up transformer is required:

$$n = \frac{V_{\mathrm{DCbus(min)}}\cdot\left(1-\varphi_{\mathrm{(min)}}/\pi\right)}{V_{\mathrm{AC(max)}}/m}, \tag{9}$$

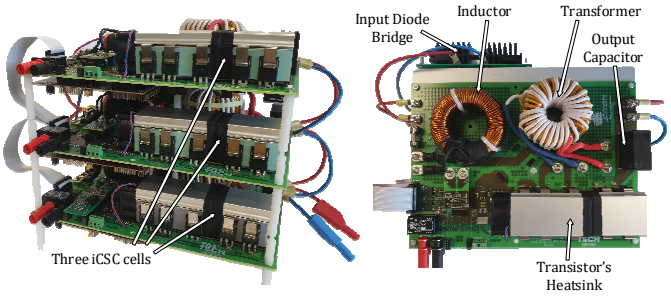
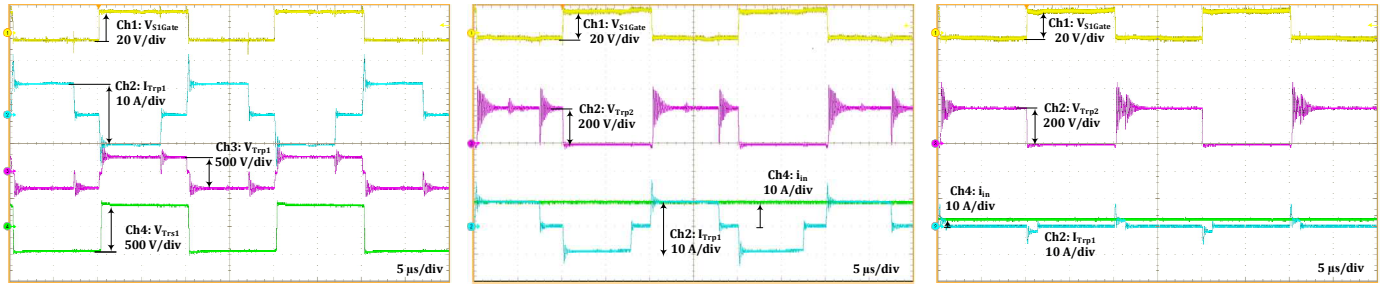


Fig. 12. Photo of the scaled prototype

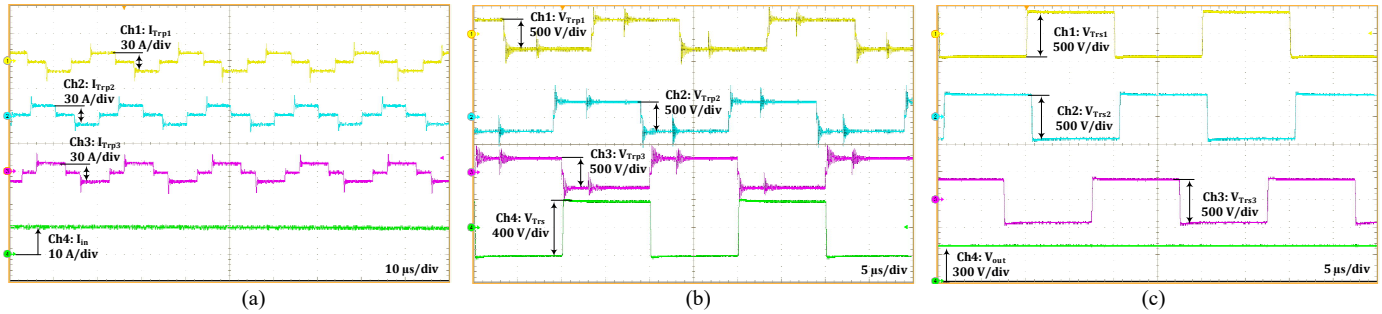
TABLE II
Specifications of the Converter Prototype

Parameter	Symbol	Value
DC-side voltage	V_{DCbus}	350…450 V
AC-side voltage	V_{AC}	440 V_{rms}
Switching frequency	f_{sw}	50 kHz
Transformer turns ratio	n	1:1.47
Maximum power	P_{rated}	4 kW
Cell capacitor (DC-side)	C_{DCbus}	40 µF
Inductors (AC-side)	$L_{1\ldots3}$	450 µH
Bridge diodes	D_1-D_4	VS-90EPF12L-M3
Input-side Transistors	S_1-S_4	C3M0120090D
Output-side Transistors	S_5-S_8	C3M0280090D
Microcontroller	-	TMS320F28379D



(a) (b) (c)

Fig. 13. Transformer primary/secondary voltages and currents (a); transformer waveforms when i_{in} is close to maximum (b) and zero (c).

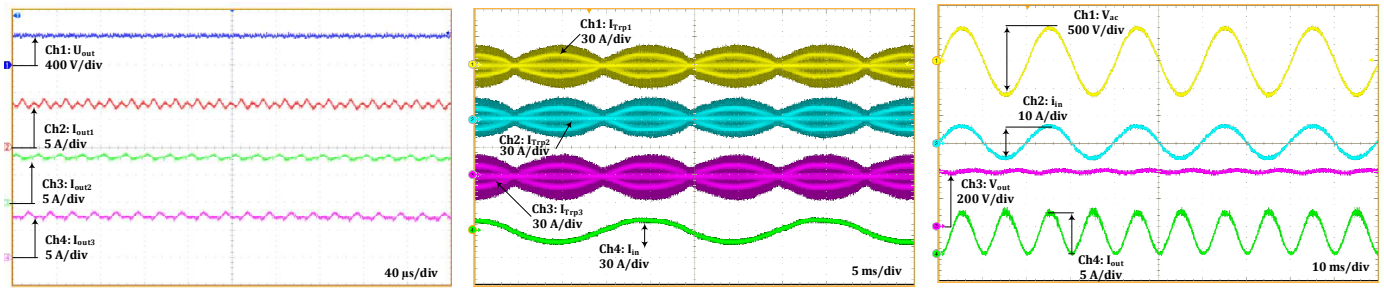


(a) (b) (c)

This work is licensed under a Creative Commons Attribution 4.0 License. For more information, see https://creativecommons.org/licenses/by/4.0/

This article has been accepted for publication in IEEE Transactions on Transportation Electrification. This is the author's version which has not been fully edited and content may change prior to final publication. Citation information: DOI 10.1109/TTE.2024.3399329

Fig. 14. Transformer primary currents of cells and input current (a); transformer primary voltages of cells (b); transformer secondary voltages of cells (c).



(a) (b) (c)

Fig. 15. Output voltage and cell currents (a); transformer primary currents of cells and input current (b); input/output voltages and currents, output current of a cell (c).

The experimental waveforms of the iCSC cell are depicted in Fig. 13 - Fig. 15. As depicted in Fig. 13a, the transformer waveforms follow the theoretical ones for ASMC topology and are not distorted by the ISOP operation. Fig. 13b and c demonstrate how the topology manages regulation of the active state and variation of peak current following the instantaneous input current using (2). The balanced currents and voltages of the cells are presented in Fig. 14. As observed, transformer voltages and currents are naturally balanced without additional control loops. The absence of interleaving between the cells can also be noticed. Fig. 14a demonstrates the currents of the cells' transformers. They follow the sinusoidal envelope, and thanks to the introduced variation of the duty cycle, the current circulation is minor. The transformer primary and secondary voltages are depicted in Fig. 14b and c, and the output currents of cells are given in Fig. 15a. The converter provides PFC with a sinusoidal shape of the input current (Fig. 15b). Due to the absence of dc-link, the output current of the cell has 100 Hz pulsations (Fig. 15c), closely following the simulated waveforms from Fig. 6. As already mentioned, the full charging station is considered to have the three-phase input connection (see Fig. 1). If the outputs of all phases are connected in parallel, the problem of second harmonic will be eliminated. The demonstrator showed an efficiency of 94.5%. The relatively low values can be explained by the series connection of cells with the voltage-overrated SiC MOSFETs that have been used in the prototype. The authors intended to apply the SiC technology comparable to the one intended for the full system and not to use lower voltage Si devices with different dynamics that are otherwise suitable for the test voltages available.

VI. Discussion and Conclusions

The shift to EV technology requires significant developments of associated charging infrastructure. To improve the EV users' comfort level, the number of fast charging stations needs to be increased, particularly in locations with a strong grid connection. This paper presented SST-type modular technology for a fast EV charging station that is supplied from the MV ac grid. Similar to other existing SST-based concepts, the use of high-frequency transformers allows for reducing the installation size and weight, while the modularity principle allows using widely available discrete semiconductor components and provides flexibility and desired redundancy.

At the same time, the proposed technology applies the ISOP connection of isolated current-source type cells in ac-dc PFC application for the first time. Such a combination provides unique features innate only to this connection. Compared to other solutions, it provides the following advantages:

- eliminates the need for bulky dc-link capacitors that otherwise make up for a significant portion of system cost and volume;
- in contrast to the voltage-source type systems, the voltage balancing of the cells is achieved naturally, without the need for additional sensing and control loops;
- features better fault tolerance and significantly reduced sensing and communication requirements between the cells, simplifying the system and reducing its cost.

At the same time, a few comments should be given regarding the specifics of the concept. The design endorses the use of transformers with minimized leakage inductance value. Although the system can be easily designed with transformers having a low turns ratio (which simplifies the achievement of reduced leakage inductance), the full isolation requirement can still put some restrictions on this aspect. Another problem is related to the well-known problem of voltage oscillations on the primary side that is common to iCSCs. Despite solving the problem of large voltage overshot with modulation, additional measures in the reduction of voltage stress, like the use of small snubber/clamp circuits, will probably be required to improve the feasibility of the solution. The concept did not utilize interleaving techniques to avoid high-bandwidth communication links. Evidently, the interleaving can improve the utilization of input filter inductors; however, the feasibility in terms of cost will depend on the particular case and has to be evaluated separately.

The scaled experimental prototype has verified and confirmed the properties of the proposed iCSC-based MCB system. It can be viewed as a potential alternative to conventional two-stage MV FCS configurations with dc-link, bringing important benefits in terms of scalability, simplicity of control, and low communication requirements, while keeping the other advantages of MCB topologies.

This work is licensed under a Creative Commons Attribution 4.0 License. For more information, see https://creativecommons.org/licenses/by/4.0/

This article has been accepted for publication in IEEE Transactions on Transportation Electrification. This is the author's version which has not been fully edited and content may change prior to final publication. Citation information: DOI 10.1109/TTE.2024.3399329

REFERENCES

[1] "Zero emission vehicles: first 'Fit for 55' deal will end the sale of new CO2 emitting cars in Europe by 2035", European Commission Press Relaease, Brussels, 28 Oct. 2022 [Online]. Available: https://ec.europa.eu/commission/presscorner/detail/en/ip_22_6462 (Accessed 19 March 2024)

[2] Order, Executive. "14037 of August 5, 2021,"Strengthening American Leadership in Clean Cars and Trucks,"." Federal Register 86.151 (2021): 43583-43585.

[3] Europe Electric Vehicle Charging Stations Market - Industry Trends and Forecast to 2029", Report, Data Bridge Market Research, [Online] Available www.databridgemarketresearch.com/reports/europe-electric-vehicle-charging-stations-market [Accessed: 19 March 2024].

[4] 2Zero Partnership 2021-2027, "Strategic research and innovation agenda", European Commission, Dec 2021. [Online] Available: https://www.2zeroemission.eu/wp-content/uploads/2021/12/2021-2Zero-SRIA-FINAL-1.pdf [Accessed: 19 March 2024].

[5] IEA (2022), Global EV Outlook 2022, IEA, Paris https://www.iea.org/reports/global-ev-outlook-2022 , License: CC BY 4.0 [Accessed: 19 March 2024].

[6] T. -T. LE, R. M. Hakim and S. Choi, "A High-Efficiency Bidirectional Single-Stage AC-DC Converter Under Wide Voltage Range for Fast Chargers," in IEEE Transactions on Power Electronics, vol. 38, no. 4, pp. 4945-4956, April 2023, doi: 10.1109/TPEL.2022.3230404.

[7] D. Rothmund, G. Ortiz and J. W. Kolar, "SiC-based unidirectional solid-state transformer concepts for directly interfacing 400V DC to Medium-Voltage AC distribution systems," 2014 IEEE 36th International Telecommunications Energy Conference (INTELEC), Vancouver, BC, Canada, 2014, pp. 1-9, doi: 10.1109/INTLEC.2014.6972199.

[8] L. Camurca, T. Pereira, F. Hoffmann and M. Liserre, "Analysis, Limitations, and Opportunities of Modular Multilevel Converter-Based Architectures in Fast Charging Stations Infrastructures," in IEEE Transactions on Power Electronics, vol. 37, no. 9, pp. 10747-10760, Sept. 2022, doi: 10.1109/TPEL.2022.3167625.

[9] M. Kasper, D. Bortis, G. Deboy and J. W. Kolar, "Design of a Highly Efficient (97.7%) and Very Compact (2.2 kW/dm^3) Isolated AC–DC Telecom Power Supply Module Based on the Multicell ISOP Converter Approach," in IEEE Transactions on Power Electronics, vol. 32, no. 10, pp. 7750-7769, Oct. 2017, doi: 10.1109/TPEL.2016.2633334.

[10] M. Lee, C. -S. Yeh, O. Yu, J. -W. Kim, J. -M. Choe and J. -S. Lai, "Modeling and Control of Three-Level Boost Rectifier Based Medium-Voltage Solid-State Transformer for DC Fast Charger Application," in IEEE Transactions on Transportation Electrification, vol. 5, no. 4, pp. 890-902, Dec. 2019, doi: 10.1109/TTE.2019.2919200.

[11] F. Wang, G. Wang, A. Huang, W. Yu and X. Ni, "Design and operation of A 3.6kV high performance solid state transformer based on 13kV SiC MOSFET and JBS diode," 2014 IEEE Energy Conversion Congress and Exposition (ECCE), 2014, pp. 4553-4560.

[12] . Ortiz and J. W. Kolar, "Solid-state-transformers: Key components of future traction and smart grid systems," in Proc. Int. Power Electron. Conf., Hiroshima, Japan, May 2014, pp. 22–35.

[13] F. Hoffmann, L. Camurca and M. Liserre, "Modular EV Fast Charging Station Architectures based on Multiphase-Medium-Frequency Transformer," IECON 2018 - 44th Annual Conference of the IEEE Industrial Electronics Society, Washington, DC, USA, 2018, pp. 1327-1332, doi: 10.1109/IECON.2018.8591772.

[14] S. Srdic, C. Zhang, X. Liang, W. Yu, and S. Lukic, "A SiC-based power converter module for medium-voltage fast charger for plug-in electric vehicles," in Proc. IEEE Appl. Power Electron. Conf. Expo. (APEC), Mar. 2016, pp. 2714-2719.

[15] N. Hugo, P. Stefanutti, M. Pellerin and A. Akdag, "Power electronics traction transformer," 2007 European Conference on Power Electronics and Applications, Aalborg, Denmark, 2007, pp. 1-10, doi: 10.1109/EPE.2007.4417649.

[16] N. D. Dao, H. V. Nguyen and D. -C. Lee, "Semi-Modular Solid-State Transformers With Reduced Count of Components Based on Single-Stage AC/DC Converters," in IEEE Transactions on Power Electronics, vol. 37, no. 7, pp. 8177-8189, July 2022, doi: 10.1109/TPEL.2022.3152501.

[17] A. Blinov, A. Chub, D. Vinnikov and S. Bayhan, "Single-Stage Series-Connected Isolated Converters for MVAC to DC Applications," 2022 3rd International Conference on Smart Grid and Renewable Energy (SGRE), Doha, Qatar, 2022, pp. 1-4, doi: 10.1109/SGRE53517.2022.9774185.

[18] Y. Zeng et al., "Autonomous Input Voltage Sharing Control and Triple Phase Shift Modulation Method for ISOP-DAB Converter in DC Microgrid: A Multiagent Deep Reinforcement Learning-Based Method," in IEEE Transactions on Power Electronics, vol. 38, no. 3, pp. 2985-3000, March 2023, doi: 10.1109/TPEL.2022.3218900.

[19] J. Shi, W. Gou, H. Yuan, T. Zhao and A. Q. Huang, "Research on voltage and power balance control for cascaded modular solid-state transformer," in IEEE Transactions on Power Electronics, vol. 26, no. 4, pp. 1154-1166, April 2011, doi: 10.1109/TPEL.2011.2106803.

[20] A. Mohammadpour, L. Parsa, M. H. Todorovic, R. Lai, R. Datta and L. Garces, "Series-Input Parallel-Output Modular-Phase DC–DC Converter With Soft-Switching and High-Frequency Isolation," in IEEE Transactions on Power Electronics, vol. 31, no. 1, pp. 111-119, Jan. 2016, doi: 10.1109/TPEL.2015.2398813.

[21] A. Blinov, R. Kosenko, D. Vinnikov and L. Parsa, "Bidirectional Isolated Current-Source DAB Converter With Extended ZVS/ZCS Range and Reduced Energy Circulation for Storage Applications," in IEEE Transactions on Industrial Electronics, vol. 67, no. 12, pp. 10552-10563, Dec. 2020, doi: 10.1109/TIE.2019.2958291.

[22] D. Zinchenko, A. Blinov, A. Chub, D. Vinnikov, I. Verbytskyi and S. Bayhan, "High-Efficiency Single-Stage On-Board Charger for Electrical Vehicles," in IEEE Transactions on Vehicular Technology, vol. 70, no. 12, pp. 12581-12592, Dec. 2021, doi: 10.1109/TVT.2021.3118392.

[23] A. Blinov, R. Kosenko, A. Chub and D. Vinnikov, "Snubberless boost full bridge converters: Analysis of soft switching performance and limitations", Int. J. Circ. Theor. Appl, pp. 1-25, 2019.

[24] A. Blinov, I. Verbytskyi, D. Peftitsis and D. Vinnikov, "Regenerative Passive Snubber Circuit for High-Frequency Link Converters," in IEEE Journal of Emerging and Selected Topics in Industrial Electronics, vol. 3, no. 2, pp. 252-257, April 2022, doi: 10.1109/JESTIE.2021.3066897.

[25] I. Verbytskyi, A. Blinov, P. Emiliani and I. Galkin, "Digital Control of PFC Rectifier with Combined Feedforward and PI Regulator," IECON 2022 – 48th Annual Conference of the IEEE Industrial Electronics Society, Brussels, Belgium, 2022, pp. 1-6, doi: 10.1109/IECON49645.2022.9968509.

This work is licensed under a Creative Commons Attribution 4.0 License. For more information, see https://creativecommons.org/licenses/by/4.0/